miR-132 regulates the differentiation of dopamine neurons by directly targeting Nurr1 expression

Dehua Yang[1,2,*], Ting Li[1,*], Yi Wang[1], Yuanjia Tang[1], Huijuan Cui[1], Yu Tang[1], Xiaojie Zhang[1], Degui Chen[3], Nan Shen[1] and Weidong Le[1,2,4,‡]

[1]Key Laboratory of Stem Cell Biology, Institute of Health Sciences, Shanghai Institutes for Biological Sciences, Chinese Academy of Sciences, Shanghai Jiao Tong University School of Medicine, 225 South Chongqing Road, Shanghai, 200025, China
[2]Institute of Neurology, Ruijin Hospital, Shanghai Jiao Tong University School of Medicine, 197 Rui Jin Er Road, Shanghai 200025, China
[3]Institute of Biochemistry and Cell Biology, Shanghai Institutes for Biological Sciences, Chinese Academy of Sciences, 320 Yue Yang Road, Shanghai, 200031, China
[4]Department of Neurology, Baylor College of Medicine, 6501 Fannin St., NB320, Houston, Texas 77030, USA
*These authors contributed equally to this work
‡Author for correspondence (weidongl@bcm.edu)

Accepted 21 November 2011
Journal of Cell Science 125, 1673–1682

doi: 10.1242/jcs.086421

Summary

Although it is well established that embryonic stem (ES) cells have the potential to differentiate into dopamine neurons, the molecular basis of this process, particularly the role of microRNAs (miRNAs), remains largely unknown. Here we report that miR-132 plays a key role in the differentiation of dopamine neurons by directly regulating the expression of Nurr1 (also known as nuclear receptor subfamily 4 group A member 2; Nr4a2). We constructed a mouse ES cell line CGR8, which stably expresses GFP under the tyrosine hydroxylase (TH) promoter, so the TH-positive neurons could be easily sorted using fluorescence-activated cell sorting (FACS). Then, we performed a miRNA array analysis on the purified TH-positive neurons and found that 45 of 585 miRNAs had more than a fivefold change in expression level during dopamine neuron differentiation. Among the 45 miRNAs, we were particularly interested in miR-132 because this miRNA has been reported to be highly expressed in neurons and to have a potential role in neurodegenerative diseases. We found that the direct downregulation of endogenous miR-132 induced by miR-132 antisense oligonucleotide (miR-132-ASO) promoted the differentiation of TH-positive neurons, whereas ectopic expression of miR-132 in ES cells reduced the number of differentiated TH-positive neurons but did not change the total number of differentiated neurons. Furthermore, we identified that miR-132-ASO could substantially reverse the miR-132-mediated suppression of TH-positive neuron differentiation. Moreover, through a bioinformatics assay we identified the Nurr1 gene as a potential molecular target of miR-132. Using a luciferase-reporter assay and western blot analysis, we demonstrated that miR-132 could directly regulate the expression of Nurr1. Collectively, our data provide the first evidence that miR-132 is an important molecule regulating ES cell differentiation into dopamine neurons by directly targeting Nurr1 gene expression.

Key words: Embryonic stem cell, MicroRNA, miR-132, Nurr1, Dopamine neuron

Introduction

Dopamine neurons are present in many regions in the central nervous system with the largest population in the midbrain, and they play important roles in motor function, emotional behavior, natural motivation and reward (Bjorklund and Dunnett, 2007). Midbrain dopamine neuron degeneration is a hallmark of Parkinson's disease (PD) (Weidong et al., 2009). Thus, an in-depth examination of the molecular pathways underlying dopamine neuron development is crucial for understanding the pathogenesis of PD and for testing the potential of stem cell therapy for this disease. Embryonic stem (ES) cells are pluripotent cells that can be induced to differentiate into all cell types of an organism and that have the potential to be used in cell replacement therapy (Roy et al., 2006). ES cell differentiation in vitro provides a powerful research tool for the genetic profiling of dopamine neuron development and cell biology. In recent years, several laboratories have investigated the mechanism of differentiation of ES cells to dopamine neurons and have identified a few regulatory factors that influence the emergence of dopamine neurons during ES cell differentiation (Prakash and Wurst, 2006). However, the molecular mechanisms underlying the dopamine neuron differentiation process are still largely unknown. Furthermore, emerging evidence shows that noncoding RNAs, including microRNAs (miRNAs), which form part of the post-transcriptional machinery, have an important role in modulating mRNA decay and translation rates in eukaryotes (Lim et al., 2003). The combination of these diverse regulatory processes on protein expression and activity allows for a wide range of cellular responses to changes in the local environment.

miRNAs are a class of small, noncoding RNAs of 21–23 nucleotides that regulate gene expression at the post-transcriptional level by binding to the mRNA of protein coding genes (Du and Zamore, 2007). Specifically, the 'seed' region of a miRNA (centered on nucleotides 2–7) binds to the 3′ untranslated region (UTR) or the open reading frame (ORF) of target mRNAs by Watson–Crick complementary base pairing (Yekta et al., 2004). Subsequently, these target mRNAs are most commonly repressed by Argonaute-catalyzed cleavage and/or destabilization. miRNAs play important roles in many cellular processes, including stem cell differentiation and maintenance,

and neural lineage specification (Hatfield et al., 2005; Houbaviy et al., 2003; Judson et al., 2009). However, there have been only a few studies on the specific miRNAs expressed in ES-cell-differentiated dopamine neurons (Kim et al., 2007; Leucht et al., 2008). This information is crucial because miRNAs could be potential key regulators of dopamine neuron differentiation (Hebert and De Strooper, 2007; Leucht et al., 2008). In fact, miRNA-deficient mice, such as those with Dicer deletions, display considerable impairment in dopamine neuron differentiation, oligodendrocyte differentiation and myelin formation (Hebert and De Strooper, 2007; Kawase-Koga et al., 2009; Leucht et al., 2008; Shin et al., 2009).

To identify miRNAs specifically expressed in dopamine neurons and determine their roles in neuronal differentiation, we stably transfected mouse ES cell line CGR8 with a tyrosine hydroxylase (TH)-promoter-driven GFP reporter, and purified TH-positive cells from the stably transfected ES cells using fluorescence-activated cell sorting (FACS). We then examined the miRNA profiles of the FACS-purified TH-positive cells, the TH-negative cells and neural progenitors using an ABI TaqMan probe. The miRNAs with the largest changes in expression levels in the differentiated TH-positive cells as compared with TH-negative cells and neuronal progenitor cells were selected, and among them we identified miR-132 as a previously unknown regulator in dopamine neuron differentiation. Using bioinformatics and molecular biological analysis, we demonstrated that miR-132 can directly regulate the expression of Nurr1, which is one of the most important transcription factors in determining dopamine neuron development and differentiation (Jankovic et al., 2005; Saucedo-Cardenas et al., 1998). Furthermore, we documented the interaction between Nurr1, brain-derived neurotrophic factor (BDNF) and miR-132 in the differentiating dopamine neurons.

Results

Derivation of dopamine neurons from mouse ES cells stably transfected with TH-GFP reporter

To better obtain stably differentiated dopamine neurons from ES cells, we modified the stromal cell-derived inducing activity (SDIA) method by plating the ES-cell-derived embryoid bodies (EBs) onto PA6 cells. Using our modified SDIA method we found that almost all the clones showed TH-positive dopamine neurons after 14 days of differentiation (Fig. 1A–D).

For the selection of ES cells stably integrating the TH–GFP sequence, we used two steps to identify clones expressing both TH and GFP. First, after transiently transfecting the plasmids into CGR8 cells and culturing for 14 days with the antibiotic G418, we selected 50 G418-resistant clones for analysis of GFP integration by genomic DNA PCR. Of the 50 clones selected, 31 clones integrated GFP, and of these, we selected the 10 clones with the highest GFP. We then expanded these 10 clones and differentiated them into dopamine neurons by co-culturing them with PA6 cells for 13 days. Using immunocytochemistry and GFP fluorescence, we selected clone no. 48 which had the highest level of TH–GFP co-expression (Fig. 2) for further study.

miRNA profiles of GFP-positive cells, GFP-negative cells and neural progenitor cells

FACS analysis was employed to further characterize clone no. 48. Following in vitro differentiation for 13 days, the clone cells were sorted by FACS, and more than 90% of the resulting cells were GFP-positive (Fig. 3A). FACS analysis showed that the dopamine neuron differentiation from clone no. 48 contained a significantly higher number of GFP-positive cells [4.1%±0.4% (n=3)].

To confirm the gene expression of dopamine-related markers in the GFP-positive dopamine neurons, GFP-negative cells and neural progenitor cells, we extracted total RNAs from these cells and analyzed the mRNA expression using real-time PCR. Fig. 3B shows that the TH gene expression was dramatically upregulated in the GFP-positive cells, confirming that TH is co-expressed with GFP. In addition to TH expression, the other important dopamine-related genes, including those for Nurr1, Pitx3, BDNF and GDNF, were all significantly (P<0.01) upregulated in GFP-positive cells by approximately 14-, 4-, 14- and 4-fold, respectively (Fig. 3C–F). Nurr1 protein expression also showed the same increase as the mRNA (supplementary material Fig. S5). We then detected the expression of nestin, a marker of neural stem cells, which was found to be highly expressed in neural

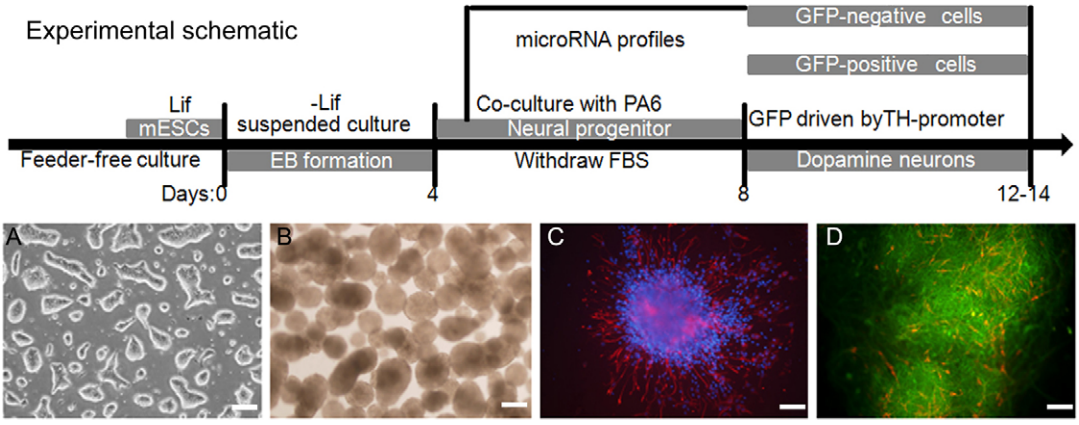

Fig. 1. A schematic of the experimental procedure for dopamine neuronal differentiation and miRNA profiling, and phase-contrast and fluorescence images of cells at different stages of dopamine neuron differentiation in mouse ES cells. Top: experimental procedure. (**A**) Mouse ES cells (CGR8 cell line) maintained in the presence of LIF. (**B**) Day 0: ES cells were dissociated from a gelatin-coated dish. Initial differentiation was induced by the formation of EBs for 4 days, followed by neural induction by co-culturing with PA6 cells. (**C**) Days 4–8: nestin-positive (red) neural progenitors appeared. (**D**) Days 8–14: dopamine neurons developed that were stained with TH (red) and MAP2 (green). We selected the GFP-positive cells, GFP-negative cells and neural progenitors to analyze the miRNA profiles. Scale bars: 100 μm.

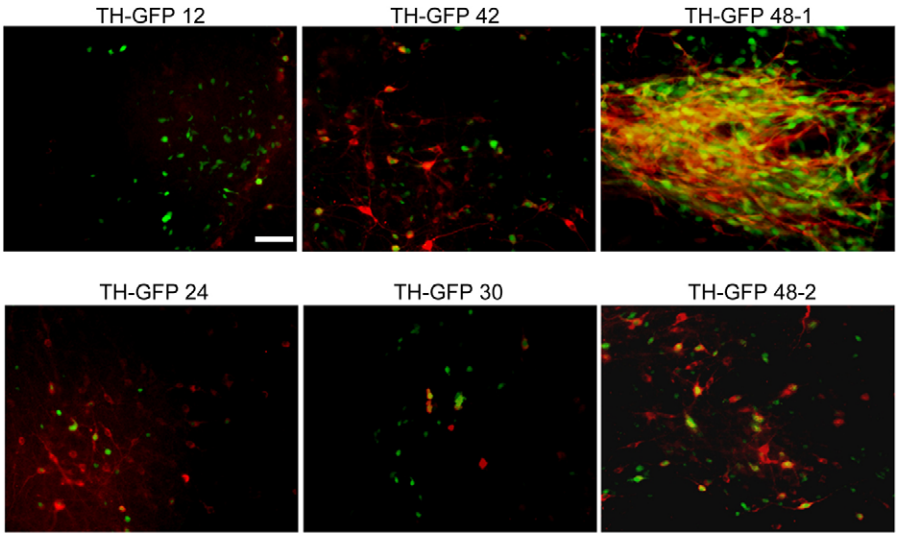

Fig. 2. Evaluation of TH–GFP constructs in mouse ES cells during in vitro differentiation. We evaluated G418-resistant clones by in vitro differentiation and immunocytochemistry. The staining of the five 9-kb TH–GFP clones (12, 24, 30 42 and 48) showed that TH–GFP 48 had the most overlap (~70% overlap) in GFP fluorescence (green) and TH staining (red). TH–GFP 48-1 showed dopamine neuron differentiation at higher cell density, whereas TH-GFP48-2 showed differentiation at lower cell density. All differentiation experiments were performed twice. Scale bar: 100 μm.

progenitor cells (supplementary material Fig. S3). We also replated the sorted GFP-positive cells into cell culture flasks and observed the GFP expression using fluorescent microscopy, which showed that more than 90% of the cells were GFP positive (Fig. 3A).

Using the TaqMan Low Density Assay v2.0 (Applied Biosystems), we assayed the miRNA expression profiles of the FACS sorted GFP-positive cells, GFP-negative cells and neural progenitor cells. Of the 585 mouse miRNAs, 45 showed a more than fivefold increase in expression in the GFP-positive cells compared with GFP-negative cells and/or neural progenitor cells. Among the 45 miRNAs, 17 miRNAs including miR-132 have been reported to be expressed in the central nervous system (Chen et al., 2010; Junn et al., 2009; Kim et al., 2007; Leucht et al., 2008; Schratt et al., 2006; Sempere et al., 2004; Shioya et al., 2010; Smrt et al., 2010; Zhao, C. et al., 2010) and they have been known to function in neural proliferation, differentiation or protection (Table 1). We then verified the change of miR-132 expression by real-time PCR amplification and found that the miR-132 expression in TH-positive cells was approximately tenfold and fivefold greater than in GFP-negative cells and neural progenitor cells, respectively, which was consistent with the miRNA expression profiles determined by the TaqMan Low Density Assay (Fig. 4A). In addition, using the standard curve based on the chemical synthesis of miR-132 (supplementary material Fig. S1), we measured the absolute levels of the mature miR-132 in GFP-positive cells, GFP-negative cells and neural progenitor cells, which were 0.13 fmol, 0.034 fmol and 0.023

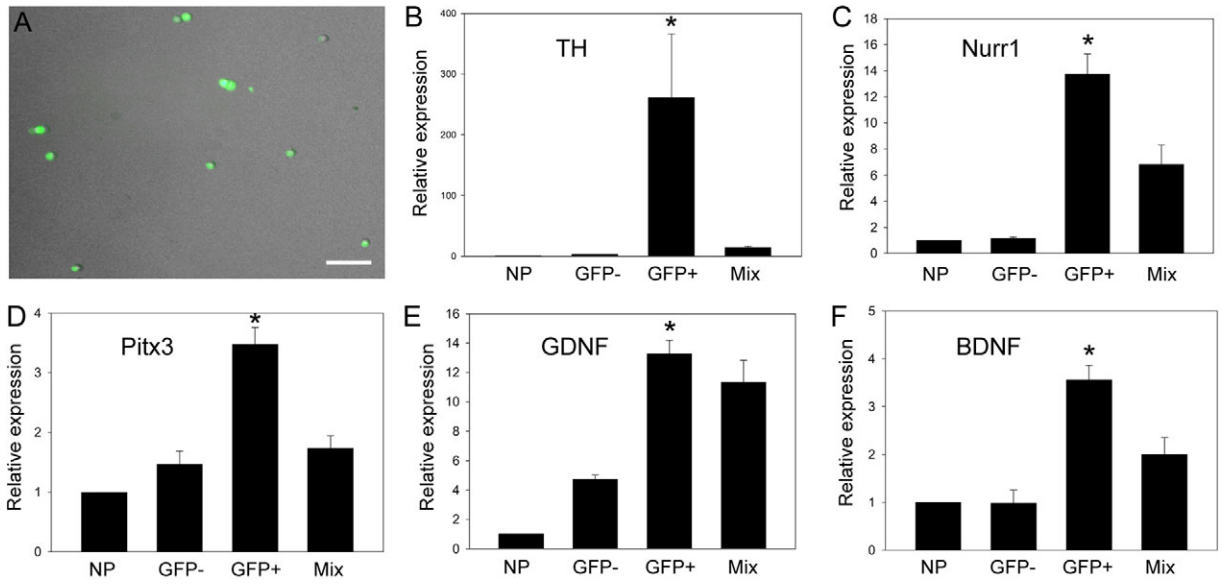

Fig. 3. Identification of the FACS-sorted GFP-positive cells. TH-GFP48 cells were differentiated for 13 days, and then dissociated and sorted by FACS. (**A**) More than 90% of the sorted cells were GFP positive (GFP+) under the fluorescence microscope, following replating of cells in a 24-well plate. (**B**–**F**) We detected the expression of genes of dopamine neuron-related markers by real-time PCR. The gene expression of TH (B), Nurr1 (C), Pitx3 (D), BDNF (E) and GDNF (F) was significantly upregulated in the GFP-positive cells (GFP+) compared with neural progenitors (NP), GFP-negative cells (GFP–) and the unsorted cells (Mix) after 14 days of differentiation in vitro. All real-time PCR experiments were performed three times in duplicate. *P<0.01. Scale bar: 100 μm.

Table 1. The relative expression of a sample of miRNAs based on the miRNA profiles of the three different cell types

microRNAs	GFP positive	GFP negative	Neural progenitor
mmu-let-7a*	1	1.00	10.00
mmu-let-7b	1	0.84	5.14
mmu-miR-10a	1	0.16	0.04
mmu-miR-124	1	0.15	0.07
mmu-miR-128a	1	0.19	0.13
mmu-miR-132	**1**	**0.09**	**0.21**
mmu-miR-133b	1	0.04	0.07
mmu-miR-137	1	0.02	0.09
mmu-miR-21	1	0.31	5.59
mmu-miR-214	1	1.22	5.22
mmu-miR-218	1	0.23	0.09
mmu-miR-29a	1	0.64	7.51
mmu-miR-29b	1	0.33	7.00
mmu-miR-302a	1	0.86	6.72
mmu-miR-302b	1	2.66	11.69
mmu-miR-7a	1	1.62	9.85
mmu-miR-9	1	0.29	0.13
SnoRNA429	1	1.00	0.99
SnoRNA202	1	1.00	1.01

fmol per 2 μg total RNA, respectively. Therefore, the absolute levels of miR-132 in GFP-positive cells was more than fivefold higher than in neural progenitor cells. We therefore selected miR-132 for further investigation.

Examination of the roles of miR-132 in dopamine neuron differentiation

To identify the function of miR-132 in dopamine neuron differentiation, we transiently transfected miR-132 mimics into the TH-GFP-expressing ES cells on day 5 of differentiation. Three days after transfection, we found that miR-132 mimics suppressed dopamine neuron differentiation, compared with control mimics (Fig. 4C; supplementary material Fig. S4B). The number of dopamine neurons in the miR-132-transfected cells was also significantly ($P<0.05$) lower than in control cells even after 14 days of differentiation. We then transfected synthesized miR-132-ASO to further verify the effect of downregulation of endogenous miR-132 on the differentiation of dopamine neurons. The specific inhibition of miR-132-ASO on the expression of miR-132 is shown in (supplementary material Fig. S2). As shown in (Fig. 4B,C; supplementary material Fig. S4A), addition of miR-132-ASO to the cultures significantly ($P<0.05$) promoted the differentiation of dopamine neurons from ES cells.

Over-expressing miR-132 in ES cells reduces the differentiation of dopamine neurons whereas miR-132-ASO partially reverses this effect

To further determine the effect of miR-132 on the differentiation of dopamine neurons, we cloned the miR-132 precursor into pPyCAGIP and made stably transfected ES cells. By RT-PCR, we identified three clones that highly expressed miR-132 (Fig. 5A). We then induced differentiation of these three clones into dopamine neurons by co-culturing them with PA6 cells and detected the GFP fluorescence under a fluorescence microscope after 9 and 10 days of differentiation. As shown in (Fig. 5B), miR-132 strongly inhibited GFP expression compared with the stable clones expressing the empty vector. Furthermore, after the miR-132-expressing clones had differentiated for 13 days, the expression of TH and MAP2, detected by immunocytochemistry, showed a dramatic decrease in TH-positive cells in miR-132-expressing clones compared with control clones; however, there was no difference in the total number of MAP2-positive neurons (Fig. 5C; supplementary material Fig. S4C). In addition, we transiently transfected miR-132-ASO into miR-132-expressing cells after 6 days of differentiation. We found that application of miR-132-ASO could significantly ($P<0.05$) rescue the TH expression in miR-132 cells compared with negative control (Fig. 5C; supplementary material Fig. S4C).

miR-132 directly downregulates Nurr1 protein expression

To determine how miR-132 affects differentiation of dopamine neurons, we tried to identify the potential targets of miR-132 through a bioinformatics search. Notably, the bioinformatics search identified Nurr1, the key transcription factor in dopamine neuron development, as a potential target of miR-132, and we

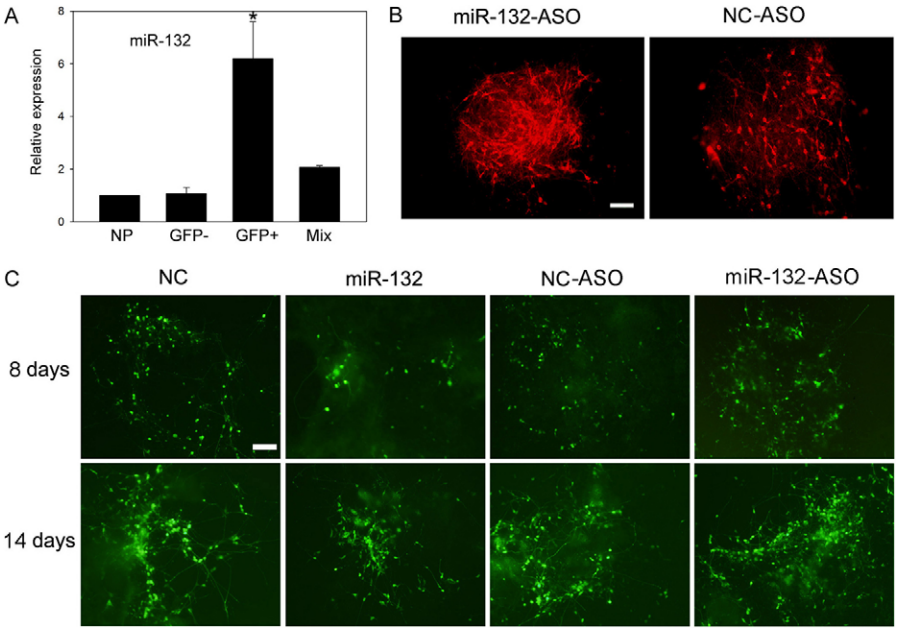

Fig. 4. Transiently transfected miR-132 suppressed the intensity of GFP fluorescence, indicating the expression of the TH gene. (**A**) Relative expression of miR-132 in cultured ES cells. The expression of miR-132 in GFP-positive (GFP+) cells was significantly higher than in GFP-negative (GFP–) cells, neural progenitors (NP) and unsorted cells (Mix), which was consistent with the result of ABI TaqMan-based miRNA profiles (Table 1). (**B**) By transiently transfecting miR-132-ASO and NC-ASO, miR-132 mimics (miR-132) and negative control (NC) on day 5 of in vitro differentiation, we found that miR-132-ASO, the inhibitor of endogenous miR-132, promoted the differentiation of dopamine neurons (determined by immunocytochemistry of TH). (**C**) Overexpression of miR-132 substantially suppressed the GFP+ cell differentiation on days 8 and 14, as compared with the NC overexpression control; whereas transient transfection of miR-132-ASO could upregulate the proportion of GFP+ cells. All real-time PCR experiments were repeated three times in duplicate. The experiments for differentiation were performed twice (*$P<0.01$). Scale bars: 100 μm.

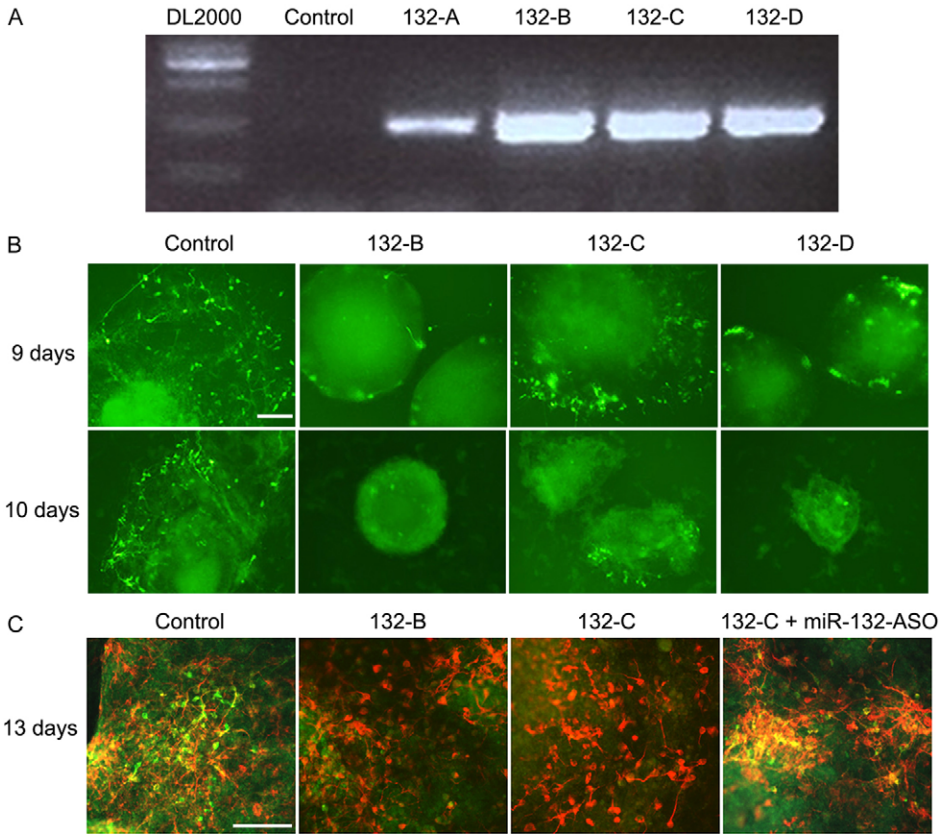

Fig. 5. The stable expression of miR-132 dramatically inhibited the appearance of TH-positive cells, whereas miR-132-ASO partially rescued this inhibition. We transfected miR-132-expressing plasmid into ES cell clone no. 48 and selected the puromycin-resistant clones after 2 weeks. (**A**) RT-PCR showed that four clones (miR-132A, miR-132B, miR-132C and miR-132D) stably expressed miR-132. Then we selected miR-132B, miR-132C and miR-132D for further studies. (**B**) Compared with the empty-vector-transfected control (control), miR-132B, C and D repressed GFP fluorescence when the ES cells were differentiated for 9 and 10 days in vitro. (**C**) After differentiation for 13 days, we stained the cells for TH and MAP2, which showed a substantial decrease in the number of TH-positive cells (green), whereas the MAP2-positive neurons (red) were not affected. In addition, we transiently transfected the miR-132-ASO into miR-132 -expressing cells (miR-132C) on day 6 of cell differentiation. miR-132-ASO could partially rescue the suppression of the differentiation of dopamine neurons by miR-132. All experiments for differentiation and staining were performed twice. Scale bars: 100 μm.

found that the binding site of Nurr1 was conserved in several species (Fig. 6A). To test whether miR-132 directly targets the binding site of Nurr1, we inserted the sequence containing the miR-132-binding site downstream of the luciferase reporter vector and co-transfected with miR-132 into HEK-293T cells. Our result demonstrated that miR-132 significantly ($P<0.01$) decreased the luciferase activity of pGL-Nurr1-expressing cells but had no effect on an empty pGL3 construct, which lacked a miR-132-binding site (Fig. 6C). To avoid the interference of endogenous expression of Nurr1 in HEK-293T cells, we repeated the experiment using SK-N-SH, a neuroblastoma cell line in which no Nurr1 expression has been documented. This effect of miR-132 on Nurr1 in a luciferase assay could be replicated in SK-N-SH cells (Fig. 6E). To confirm the predicted target sequence of miR-132 binding to Nurr1, we mutagenized the two sites of the 'seed' sequence by replacing C and T with G and A, respectively (Fig. 6A, bold type). Notably, miR-132 failed to inhibit the luciferase activity of the mutagenized Nurr1 construct (Fig. 6D,F), indicating that the predicted sequence is indeed the binding site for miR-132. Furthermore, to confirm the downregulation of Nurr1 expression by miR-132, we used a full-length Nurr1 cDNA vector. Transient transfection of miR-132 and Nurr1 into HEK-293T cells substantially inhibited the expression of Nurr1 protein (Fig. 6B), which is consistent with the result of the luciferase reporter assay (Fig. 6C–F).

The homeostatic interaction of Nurr1, BDNF and miR-132 controls TH expression and dopamine neuron differentiation

Previous studies have demonstrated that Nurr1 directly regulates BDNF and TH expression (Kim et al., 2003; Volpicelli et al., 2007), and BDNF directly regulates miR-132 expression (Klein et al., 2007; Schratt et al., 2006). To further explore the roles and molecular pathways of Nurr1, BDNF and miR-132 in dopamine neuron differentiation, we established dopamine neuron differentiation in feeder-dependent ES cells (R1) using a five-step method (Lee et al., 2000) that required 10–15 days for differentiation of neural progenitor cells into dopamine neurons (Fig. 7A). From day 2 to day 14 of differentiation the expression patterns of Nurr1 and miR-132 were inversely related (Fig. 7D), but the expression patterns of BDNF and miR-132 were similar (Fig. 7E). The dopamine neurons differentiation of miR-132-infected ES cells was significantly ($P<0.05$) less than in the ES cells infected with pLVX empty vector (Fig. 7B; supplementary material Fig. S4D), which agreed with the results in feeder-free ES cells. Nurr1 expression was downregulated by miR-132 but upregulated by miR-132-ASO (Fig. 7C). The lower panel of (Fig. 7C) show that miR-132 downregulated Nurr1 expression by 35.5% and miR-132-ASO upregulated Nurr1 expression by 24%. We also found that the addition of BDNF to the cultures from day 4 to day 8 of differentiation days elevated the expression of miR-132 (Fig. 7F), which is consistent with the result of previous studies (Klein et al., 2007; Schratt et al., 2006). However, longer exposure to BDNF resulted in less change in miR-132 (Fig. 7F). By contrast, Nurr1 expression was downregulated from day 4 to day 8 of differentiation and upregulated at day 10 of differentiation (Fig. 7F). These results suggest a the homeostatic interaction between Nurr1, BDNF and miR-132.

Discussion

The conditional knockout of Dicer has shown that miRNAs play essential roles in dopamine neuron differentiation (Kim et al.,

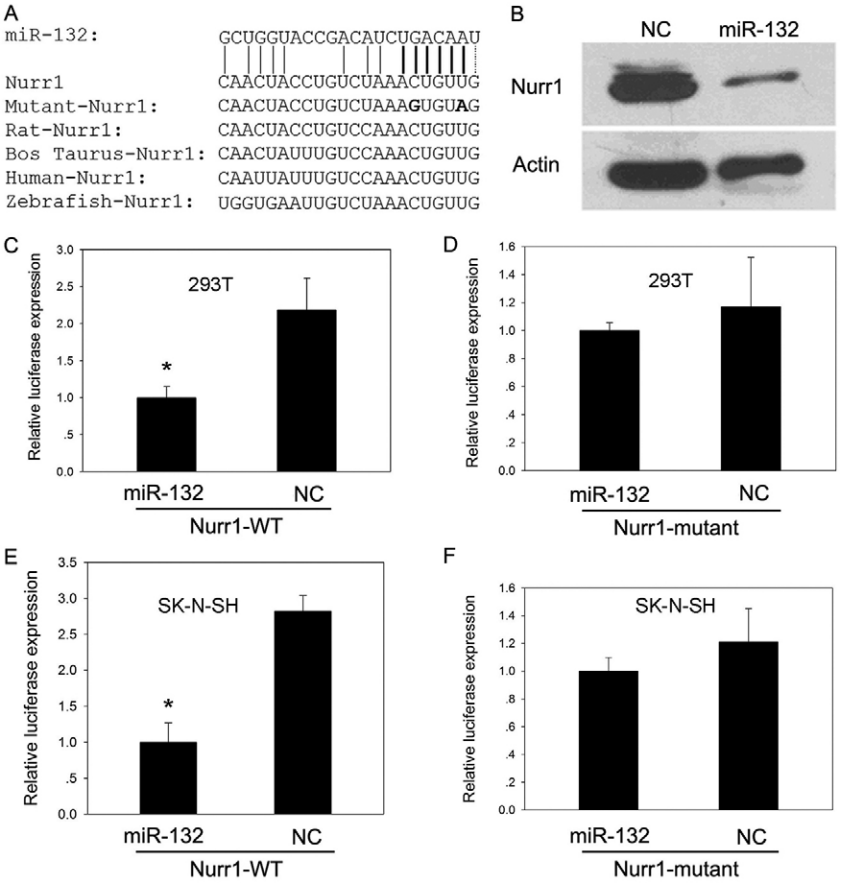

Fig. 6. Validation of Nurr1 as a direct target of miR-132 by bioinformatics, luciferase and western blot assays. (**A**) The binding site of Nurr1 and miR-132 showed that the 'seed' sequence (bold vertical bar) is conserved in the five species. The G and A shown in bold type are the binding site of the mutant form of Nurr1 for miR-132, which was cloned into a luciferase vector. (**B**) Co-transfection of miR-132 or NC and full-length Nurr1 cDNA into HEK-239T cell and analysis of protein expression by western blot assay after 48 hours demonstrated that miR-132 inhibited the expression of Nurr1 protein. (**C**–**F**) Luciferase-reporter assay in HEK-293T (C,D) and SK-N-SH (E,F) cells. (C,E) There was significant downregulation of the relative luciferase activity by miR-132 compared with NC. (D,F) The mutant miR-132 binding site of Nurr1 could not inhibit the luciferase activity. All experiments were performed three times in duplicate (*$P<0.01$).

2007). Several studies have identified a negative feedback circuit of miR-133b and Pitx3, a crucial transcription factor in dopamine neuron development (Hebert and De Strooper, 2007). These studies have also suggested that other miRNAs, in addition to miR-133b, have a function in dopamine neuron differentiation, but little is known about them (Hebert and De Strooper, 2007; Kawase-Koga et al., 2009). To document the newly identified miRNAs in dopamine neuron differentiation, we constructed a TH-promoter-derived reporter system to establish purified dopamine neurons differentiated from ES cells, and obtain their miRNA profile. To our knowledge this study is the first to establish a miRNA profile from purified dopamine neurons. The overlay of TH staining and GFP fluorescence showed that approximately 70% of the GFP-positive cells are TH-expressing dopamine neurons, which is consistent with previous studies (Hedlund et al., 2007; Yoshizaki et al., 2004). The 9-kb fragment of the rat TH promoter, including intron sequences and a poly(A) tail, could efficiently drive GFP expression in dopamine neurons differentiated from ES cells. The lack of complete overlap of TH and GFP expression could be attributed to the size of the promoter fragment or the different half-lives of TH and GFP (Hedlund et al., 2007). However, the gene expression analysis of different dopamine markers, in conjunction with previous studies, indicates that the vast majority of sorted cells are of the dopamine lineage (Yoshizaki et al., 2004; Hedlund et al., 2007).

The relative miRNA expression profiles of GFP-positive, GFP-negative and neural progenitor cells during differentiation process identified by TaqMan Low Density Assay and then confirmed by real-time PCR in our study identified several miRNAs, including miR-133b, miR-9 and miR-7, that have been reported to play a role in the central neural system, dopamine neuron development and differentiation, and have possible links to PD (Junn et al., 2009; Kim et al., 2007; Leucht et al., 2008). These results suggest that using purified dopamine neurons is of great value in the search for new miRNAs involved in dopamine neuron differentiation. We selected miR-132 for further study on the basis of a bioinformatics prediction, showing Nurr1, a crucial transcription factor for midbrain dopamine neuron development and differentiation (Kim et al., 2002; Kim et al., 2006; Luo et al., 2008), is a potential target of miR-132. miR-132 is necessary for BDNF-stimulated dendritic outgrowth (Wayman et al., 2008). Further characterization of miR-132 revealed that it can be induced by BDNF and it is able to modulate dendritic morphology through suppression of p250GTPase-activating protein (p250GAP) (Edbauer et al., 2010; Magill et al., 2010; Nudelman et al., 2010; Wayman et al., 2008). Additionally, it has been shown that miR-132 can regulate the expression of the methyl-CpG-binding protein (MeCP2), a key factor in neurodevelopment and neurological disease (Klein et al., 2007). These results further suggest an association of miR-132 with neurodevelopment and neurodegenerative diseases, such as PD. In our study, miR-132-ASO, which can inhibit the endogenous miR-132, promoted the differentiation of dopamine neurons, whereas over-expression of miR-132 dramatically repressed dopamine neuron differentiation without changing the total number of neurons. In addition, miR-132-ASO could partially

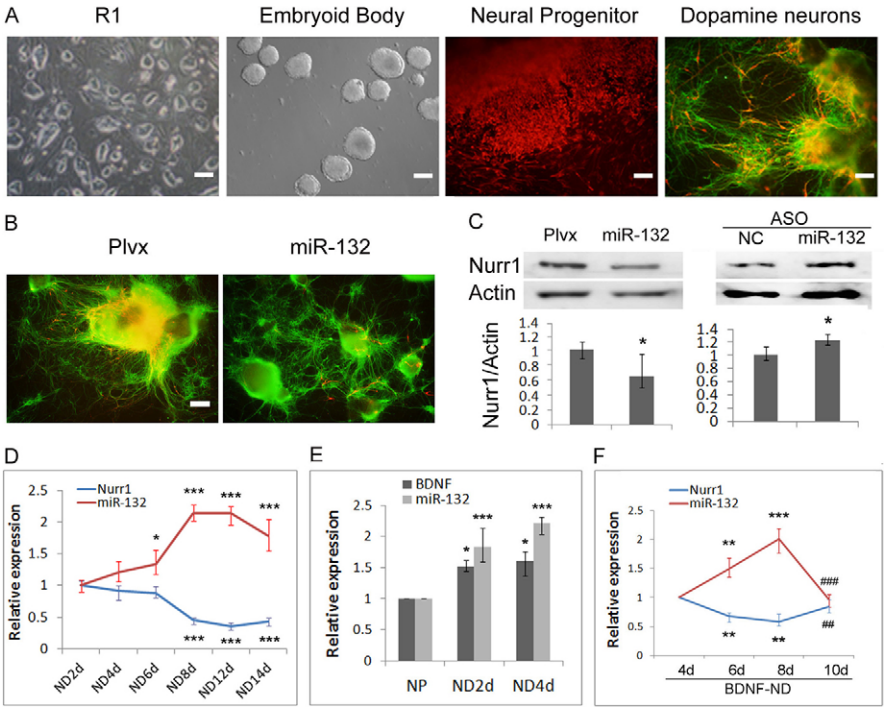

Fig. 7. The homeostatic interaction of Nurr1, BDNF, miR-132 and TH. (**A**) Five-step method for dopamine neuron differentiation. Mouse ES cells (R1 cell line) were maintained in the presence of LIF; initial differentiation was induced by the formation of EBs for 4 days followed by neural progenitor selection for 6–10 days by replating EBs and withdrawing serum; after amplification of neural progenitor for 4–6 days in the presence of bFGF, Shh and FGF8 (red: nestin), dopamine neurons were grown for 10–15 days and stained with TH (red) and MAP2 (green). (**B**,**C**) Overexpression of miR-132 by lentivirus infection dramatically inhibited the appearance of TH-positive cells [TH (red) and MAP2 (green)] by downregulating Nurr1 expression, whereas miR-132-ASO could upregulate Nurr1 expression. The lower panel of C shows the Nurr1/actin ratio determined from the western blot. We set the Nurr1/actin ratio of control (pLVX and Con-ASO) as 1. (**D**) The expression profile (from real-time PCR) of Nurr1 and miR-132 during dopamine neuron differentiation from day 2 to day 14. We set the value at day 2 as 1. (**E**) The expression of miR-132 and BDNF during the differentiation of dopamine neurons. The value of NP cells was set as 1. (**F**) In the process of dopamine neuron differentiation, BDNF were added to the medium every other day from day 4 to day 8. The results of real-time PCR showed the relative expression of Nurr1 and miR-132. The ratio of relative expression of Nurr1 and miR-132 with BDNF treatment and without BDNF treatment on the day 4 was set at 1. All experiments for differentiation and staining were performed twice and western blots were performed three times. NP, neural progenitor; ND, neuron differentiation. Scale bars: 100 μm. *$P<0.05$, **$P<0.01$ and ***$P<0.001$. compared with the control group; $^{\#\#}P<0.01$ and $^{\#\#\#}P<0.001$ in F show the value on day 10 of differentiation compared with the value on day 8.

rescue the miR-132-induced suppression of dopamine neuron differentiation, further supporting the specific suppression effects of miR-132 on dopamine neuron differentiation.

The direct regulatory effect of miR-132 on the expression of Nurr1 was further confirmed by genetic modification of the binding site of miR-132. We found that the mutation totally abolished the regulatory effect of miR-132 on Nurr1. It is well documented that Nurr1 can regulate the expression of BDNF and promote the development and maintenance of dopamine neurons (Kim et al., 2003; Volpicelli et al., 2007), whereas BDNF can induce miR-132 expression (Klein et al., 2007; Schratt et al., 2006), suggesting a potential feedback loop for Nurr1 and miR-132. We also found that in the process of dopamine neuron differentiation, the expression of Nurr1, BDNF and miR-132 continuously changed; Nurr1 and miR-132 expression patterns were inversely related, whereas that of BDNF and miR-132 were similar. The addition of BDNF caused upregulation of miR-132 and downregulation of Nurr1. Moreover, suppressing Nurr1 expression by miR-132 inhibited the expression of BDNF and further lead to the downregulation of miR-132. This lead to a new equilibrium between Nurr1 and miR-132. Together with the previous studies on the direct regulation of BDNF expression by Nurr1 and miR-132 expression by BDNF, we propose a possible homeostatic interaction between Nurr1, BDNF, miR-132 and TH, although further investigation is required to validate this finding.

Nurr1 is an orphan member of the nuclear hormone receptor superfamily of transcription factors. It is highly expressed in the ventral mesencephalon, which includes the mesencephalic dopamine neurons (Jankovic et al., 2005; Saucedo-Cardenas et al., 1998). The onset of Nurr1 expression in mesencephalic dopamine neurons is at E10.5 in the mouse, just prior to the expression of the dopamine markers TH and Pitx3 (E11.5) (Smidt et al., 2000), and expression continues into the adult stage (Weidong et al., 1999). Nurr1 is known to be essential for induction of the mesencephalic dopamine phenotype and for the survival and/or maintenance of these neurons (Kim et al., 2002; Kim et al., 2006; Luo et al., 2008). Recent studies showed that Nurr1 works in conjunction with Pitx3 to enhance the differentiation of ES cells into dopamine neurons (Jacobs et al., 2009; Martinat et al., 2006). In addition, Nurr1 is found to play a previously unexpected role in protecting these neurons from inflammation-induced neurotoxicity induced by lipopolysaccharide stimulation (Saijo et al., 2009). Interestingly, miR-132 could also be induced by lipopolysaccharide stimulation (Shaked et al., 2009). The direct effect of miR-132 on the production

of Nurr1 protein raises the possibility that miR-132 might be involved in inflammatory process of dopamine neuron degeneration in addition of its effect on dopamine neuron differentiation.

In conclusion, we report here the miRNA profiles of purified dopamine neurons using the TH-promoter-derived GFP reporter system, and we provide the first evidence that miR-132 is an important molecule that negatively regulates dopamine neuron differentiation in ES cells by directly suppressing Nurr1 expression. This finding will greatly enhance our understanding of the molecular mechanisms involved in dopamine neuron differentiation and shed new light on the generation of ES cells to be used in cell replacement therapy for PD and other neurological diseases involving dopamine neuron degeneration.

Materials and Methods

Cell culture, transfection and differentiation

All cell culture reagents and culture plastics were obtained from Gibco (Rockville, MD) and BD Biosciences (San Diego, CA), respectively, unless otherwise specified.

The mouse feeder-independent ES cell line (CGR8, early passages 19–30) was obtained from Austin Smith (Centre for Genome Research, University of Edinburgh, UK) (Ying et al., 2003) and Ying Jin (Institute of Health Sciences, Shanghai Institutes for Biological Sciences, Chinese Academy of Science) and was cultured in gelatin-coated Petri dishes without feeder cells in Glasgow minimal essential medium (GMEM) supplemented with nonessential amino acids, L-glutamine, 2-mercaptoethanol, 10% ES cell-qualified fetal bovine serum (FBS) and leukemia inhibitory factor (LIF; 1:10,000 dilution; Chemicon, Temecula, CA) in a humidified 5% CO_2 atmosphere at 37℃. Cultures were maintained at 70% confluency to maintain an undifferentiated phenotype. Cells were passaged every 2 days. Embryoid bodies (EBs) were formed in floating cultures at 2.5×10^5/ml or in hanging drop cultures at 1000 cells/20 µl for 4 days with GMEM medium without LIF. For transient transfection of miRNA mimics, negative control (NC), miR-132-ASO and NC-ASO, 150 nM of each chemical compound was transfected into ES cells using Lipofectamine 2000 (Invitrogen, Carlsbad, CA), according to the manufacturer's instructions. For stable transfection of a miR-132-expressing plasmid, the vector was transiently transfected with Lipofectamine 2000 for 24 hours and then selected using 1.5 µg/ml puromycin (Roche, Switzerland) for 2 weeks. The single clones were picked and cultured for confirmation and further experiments.

R1 mouse ES cells were cultured on mitomycin-C-treated mouse embryonic fibroblasts in Dulbecco's modified Eagle's medium supplemented with 15% FBS, 2 mM L-glutamine, 0.1 mM non-essential amino acids, 100 IU/ml penicillin and streptomycin, 55 µM β-mercaptoethanol and LIF. The five-step method for dopamine neuron differentiation was performed as described previously (Lee et al., 2000). The method for transient transfection in R1 cells was same as for CGR8 cells, which was performed on day 3 when neural prognitor cells began amplification in the presence of basic fibroblast growth factor (bFGF; R&D Systems, Minneapolis, MN). BDNF (50 ng/ml; R&D Systems) was added to the medium on day 4 of dopamine neuron differentiation.

PA6 is a stromal cell line derived from newborn mouse calvariae. PA6 cells were purchased from Riken (Tsukuba, Japan) and maintained in PA6 culture medium [α-MEM supplemented with 50 IU/ml penicillin and 50 µg/ml streptomycin (PEST) and 10% FBS (Hyclone, Logan, UT)].

SK-N-SH is a neuroblastoma cell line, which was purchased from the Cell Bank of the Chinese Academy of Science; cells were routinely cultured in DMEM supplemented with 10% FBS (Hyclone) and penicillin and streptomycin (PEST) at 37℃ in a humidified atmosphere of 95% air and 5% CO_2. When the cells reached 80–90% confluency, they were subdivided into 24-well plates with 1×10^5 cells/well for luciferase-reporter transfection and assay.

HEK-293T cells were obtained from the Cell Bank at the Chinese Academy of Science. The cells were cultured in DMEM supplemented with 10% FBS and PEST at 37℃ in a 5% CO_2 atmosphere. At ~60% confluency HEK-293T cells were transfected using Lipofectamine 2000 with varying concentrations of synthetic miRNA mimics, NC-mimics (all from Genepharma, Shanghai, China) and plasmids, according to standard protocols. They were collected at different time points after transfection for luciferase and western blot assays.

CGR8 cells were differentiated using the stromal cell-derived inducing activity (SDIA) method, in which the cells were co-cultured with PA6 cells (Kawasaki et al., 2000). The classic SDIA method of directly plating the ES cells on PA6 feeder cells did not produce consistent dopamine differentiation. We improved this method by plating the ES-cell-derived EBs on PA6 cells, which established a more stable differentiation and constant efficiency, as compared with the classic SDIA method. To differentiate ES cells in vitro, PA6 cells were plated on gelatin-coated culture dishes to make a uniform feeder monolayer 1 day before the addition of CGR8-cell-derived EBs. ES differentiation medium [GMEM supplemented with 10% knockout serum replacement (KSR), 0.1 mM nonessential amino acids, 1 mM sodium pyruvate, 0.1 mM 2-mercaptoethanol and PEST] was used in place of ES cell medium, and cells differentiated for 10 days. The culture medium was changed every other day. The efficiency of differentiation was examined using immunocytochemistry.

Plasmid construction

A Nurr1 protein expression vector was created by PCR cloning of Nurr1 cDNA using a two fragment ligation processes. Two PCR reactions were performed with the following primer sets: fragment 1: 5′-GGCAAGCTTTTTGTCCTTCGC-TGAATTACGA-3′, 5′-AGAACTGCTGGATATGTTGGGT-3′; fragment 2: 5′-GTTGGGATGGTTAAAGAAGTGG-3′, 5′-GGCTCTAGAAAAGGCAGTGAC-TCATCTCATG-3′. Then the fragments were cloned into pcDNA3.1 at the *Hin*dIII and *Bgl*II sites (Takara, Dalian, China). The expression vector of pre-miR-132 was constructed by amplification of the mouse genomic cDNA, with the following primer set: 5′- GGCAGATCTCTCGGGCACGCCTGTTCA-3′ and 5′-GGCC-TCGAGTGCCACCT CCGCAGACAC-3′, and ligated into pPyCAGIP at the *Bgl*II and *Xho*I sites (Takara).

The luciferase reporter vector containing the wild-type sequence and the miR-132 binding site was amplified by the primer set 5′-GCGGAATTCCGACA-TTTCTGCCTTCTCC-3′, 5′-GGACTGCAGAGTTTGTCAATTATTGCTGGT-G-3′, using mouse midbrain cDNA as template. The PCR fragment was cloned into the *Eco*RI and *Pst*I sites (Takara) in the pGL3 luciferase vector (Promega, Madison, WI). The mutant sequence had two mutations in the 'seed' sequence of the miR-132 binding site, which is indicated in (Fig. 6A). We designed the primers 5′-CTACCTGTCTAAAGTGTAGGGGAAGCTGCCA-3′ and 5′-TGGCAGCTTC-CCCTACACTTTAGACAGGTAG-3′ and amplified the pGL3-miR-132 plasmid. Following overnight digestion with *Dpn*I (Fermentas), the PCR products were transformed into *Escherichia coli* DH10B.

All constructs were confirmed by DNA sequencing using an ABI 3730xl DNA Analyzers (Applied Biosystems, Foster City, CA).

Lentivirus preparation

A mouse genomic DNA fragment comprising miR-132 was amplified by PCR using the following primers set: 5′-GGCGAATTCCTCGGGCACGCCTGTTCA-3′; and 5′-GGCGGATCCTGCCACCTCCGCAGACAC-3′. The amplified fragment was inserted into *Eco*RI and *Bam*HI restriction enzyme sites of lentiviral vector pLVX-EF1α-IRES-ZsGreen1.

Sequencing-verified plasmid was then transfected into 90% confluent HEK-293FT cells together with packaging plasmid psPAX2 (Addgene, Cambridge, MA) and envelope plasmid pMD2.G (Addgene; addgene.org) using the calcium phosphate transfection method. The supernatants containing virus were collected after 48 hours, then filtered through a 0.45 µm filter. Filtered supernatants were concentrated 100-fold with a PEG Virus Precipitation Kit (BioVison, Mountain View, CA) and resuspended in PBS, using the method of Tiscornia et al. (Tiscornia et al., 2006). For ES cells infection, 100 µl concentrated virus supplemented with 10 µg/ml polybrene was used to infect ES cells. After an overnight incubation, supernatants were replaced with fresh culture medium.

TH promoter engineered GFP-reporter ES cells, FACS, RNA isolation and real-time PCR

The pTH-GFP construct containing the GFP reporter expressed under the 9-kb 5′-flanking region of the rat TH gene was a kind gift of Kazuto Kobayashi (Jomphe et al., 2005; Sawamoto et al., 2001; Yoshizaki et al., 2004) (Fukushima Medical University School of Medicine, Japan). The CGR8 ES cells were co-transfected with the pTH-GFP plasmid and pCDNA3.1-neo plasmid containing antibiotic resistant gene to obtain the stable transfection line. Stably transfected cells were selected on ES medium containing 750 µg/ml G418 (Roche). We screened a large number of independent, drug-resistant colonies (50 of the smaller-sized colonies of each construct) to isolate those exhibiting a consistent coexpression pattern of TH and GFP following in vitro differentiation on PA6 cells. A few clones that were only transfected with pcDNA3.1 were selected as NCs for GFP expression. After differentiation for 13 days on PA6, the clone that had the most overlap of GFP and TH was selected for expansion.

Cells were differentiated for 13–14 days, harvested using 0.05% Trypsin–EDTA, gently dissociated into a single-cell suspension, and resuspended in a Mg^{2+}- and Ca^{2+}-free phosphate buffered-saline (PBS) solution containing PEST and 2% FBS. Final cell density was 1×10^7/ml. Samples were filtered with a 40 µm cell filter (Becton Dickinson, Franklin Lakes, NJ) and sorted immediately by BD FACSAria.

After differentiation and FACS sorting, total RNAs from ES cell-derived neural progenitors, GFP-positive neurons and GFP-negative neurons were extracted using Trizol Reagent (Invitrogen), followed by treatment with DNaseI (Promega). cDNA was obtained using 2 µg of RNA in the ReverTra Ace first-strand synthesis system for RT-PCR (Toyobo, Japan). The resulting cDNA was used as a template for the PCR reactions. To reduce non-specific signals, primers for each gene were designed using the Primer Premier software (Oxford Molecular Ltd., Oxford, UK). We selected

primer sets that yielded specific products without the presence of non-specific bands, as evaluated by gel electrophoresis. The following primer sets were chosen for semiquantitative RT-PCR and real time PCR analyses. β-actin: 5′-GGCATTGTGATGGACTCCGG-3′; 5′-TGCCACAGGATTCCATACCC-3′. TH: 5′-AGTACTTTGTGCGCTTCGAGGTG-3′; 5′-CTTGGGAACCAGGGAACCTTG′. Pitx3: 5′-CTCTCTGAAGAAGAAGCAGCG-3′; 5′-CCGAGGGCACCATGGAGGCAGC-3′. Nurr1: 5′-GTGTTCAGGCGCAGTATGG-3′; 5′-TGGCAG TAATTTCAGTGTTGGT-3′. BDNF: 5′-TGTGGACCCTGAGTTCCACCAG-3′; 5′-CTGCCCTGGGCCCATTCACG-3′. GDNF: 5′-TGTGGACCCTGAGTTCCACCAG-3′; 5′-CTGCCCTGGGCCCATTCACG-3′. Pre-miR-132: 5′-ACCGTGGCTTTCGATTGTTA-3′; 5′-GGCGACCATGGCTGTAGACT-3′.

For semiquantitative RT-PCR, PCR reactions were carried out with 1× reaction buffer, 0.8 μM of each primer and 2.5 IU Taq DNA polymerase (Fermentas, Lithuania). Samples were amplified in a Thermocycler (Bio-Rad, Hercules, CA) under the following conditions: denaturing step at 95℃ for 40 seconds; annealing step at 56–60℃ for 30 seconds; and amplification step at 72℃ for 1 minute for 26–39 cycles. cDNA templates were normalized on the basis of the actin-specific signal, and PCR cycling was adjusted so that each primer set amplified its corresponding gene product at its detection threshold, to avoid saturation effects.

We performed real-time PCR to quantify expression levels. PCR amplification was performed in a mixture of 1× real-time PCR Master Mix and 0.8 μM of each primer in a final volume of 50 μl. Thermocycling was conducted with an Opticon DNA Engine (Bio-Rad). Cycle threshold (Ct) values were determined using the Opticon Monitor 2 software and a manual fluorescence threshold for all runs, and data were exported into an Excel workbook for analysis.

The PCR reactions consisted of 45 cycles using the following temperature profile: 95℃ for 30 seconds, 56–60℃ for 30 seconds, 72℃ for 30 seconds and 79℃ for 5 seconds. The purity of each PCR product (defined as the presence of a single, specific band) was confirmed by gel electrophoresis. A standard curve was constructed using β-actin and plasmid DNA (10^2–10^7 molecules). The fluorescent signals from specific PCR products were normalized against that of the β-actin gene, and then relative values were calculated by setting the normalized value as one for each gene. Two independent samples were analyzed for each gene, and all reactions were repeated more than twice.

For the real-time PCR measurement of mature miR-132 expression in GFP-positive cells, we used the commercial reverse transcription and PCR primer kit (RiboBio, Guangzhou, China). First, we established the standard curve of miR-132 using synthesized miR-132 (supplementary material Fig. S1). Then we measured the Ct value of GFP-positive cells, primary ventral mesencephalon (VM) cultures, GFP-negative cells and neural progenitor cells by real-time PCR, and calculated the absolute levels of miR-132 according to the standard curve.

miRNA profiling using the ABI qPCR system

Total RNA was isolated using Trizol reagent (Invitrogen). RNA quality was assessed with an Agilent 2100 bioanalyzer (Agilent, Palo Alto, CA), and only samples with an RNA integrity number greater than eight were used. For the miRNA expression analysis, TaqMan Low Density Assay v2.0 (Applied Biosystems) was used to detect up to 585 mouse miRNAs using an Applied Biosystems real-time instrument, according to the manufacturer's protocol. Normalization was performed with snoRNA202 and snoRNA429 as endogenous controls. Relative expression was calculated with the comparative Ct method (Zhao, X. et al., 2010).

Dual luciferase reporter assay

The wild-type and mutant sequences, containing miR-132 binding sites, were amplified and cloned into the 3′ UTR region of the luciferase gene in the pGL3 luciferase vector (Promega), according to methods described previously. The obtained construct was co-transfected with PRLSV40 and miR-132 mimics or NC mimics (Genepharma) into HEK-293T and SK-N-SH cells, as previously described. After 48 hours, luciferase activity was determined as the average of three independent assays using the Dual-Luciferase Reporter system (Promega), according to the manufacturer's instructions.

Western blotting

Cells were harvested at different time points according to the experimental treatments and lysed for 20 minutes in freshly prepared ice-cold RIPA lysis buffer [50 mM Tris-HCl, pH 7.4; NaCl 150 mM; 1% NP40; 0.25% sodium deoxycholate; 1 mM EDTA; 1 mM Na_2VO_4; 1 mM NaF; 1 mM phenylmethylsulfonyl fluoride (PMSF); aprotinin and leupeptin 5 mg/ml each]. Lysates were then centrifuged for 20 minutes at 16,000 ***g*** at 4℃. After protein concentrations were measured using the Bradford method, 40 μg protein from each sample was loaded onto a 12% polyacrylamide gel, transferred to a polyvinylidene difluoride membrane, blocked for 1 hour in 5% non-fat milk and incubated with primary antibodies [anti-Nurr1 (Santa Cruz, CA), anti-β-actin (Sigma, St. Louis, MO)] overnight at 4℃. After being washed with Tris-buffered saline and Tween 20 (TBST), samples were incubated with peroxidase-conjugated secondary antibodies. The immunoreactions were developed using Super Signal® West Dura Extended Duration Substrate (Pierce Biotechnology, Pittsburgh, PA), and the signal was quantified by measuring the optical density of the bands.

Immunocytochemistry

Cells were fixed in 4% formaldehyde for 30 minutes, rinsed with PBS, and then incubated with blocking buffer [5% normal horse serum (Vector Labs, Burlingame, CA)] for 30 minutes. Cells for immunofluorescent staining were then incubated overnight at 4℃ with rabbit anti-TH antibody (1:1000, Chemicon), mouse anti-microtubule-associated protein 2 (MAP2) antibody (1:1000, Sigma) and mouse anti-nestin (1:800, Chemicon). After being rinsed three more times in PBS, cells were incubated with Cy3-conjugated anti-rabbit antibody (1:800) and Cy2-conjugated anti-mouse antibody (1:400; The Jackson Laboratory, Bar Harbor, ME) for 2 hours at room temperature. After being rinsed for 3× 10 minutes in PBS, cells were incubated with Hoechst for 20 minutes and examined under a fluorescence or confocal microscope.

TH-, GFP- and MAP2-positive cells were counted in a 'blind' fashion in five random optical fields per coverslip by an unrelated investigator. Experiments were performed on two independent cell cultures.

Statistical analysis

All values are shown as means ± s.e.m. Data were analyzed using one-way ANOVA followed by post-hoc LSD multiple comparisons or independent-samples *t*-test with the SPSS 13.0 program (SPSS). A *P*-value of <0.05 was considered significant.

Acknowledgements

We thank Austin Smith for CGR8 cells, Kazuto Kobayashi for the pTH-GFP construct, Guangrui Luo and Yunlan Du for their technical assistance.

Funding

This work was supported by the National Basic Research Program of China [grant number 2007CB947904 and 2010CB945200 to W.L.]; Chinese National Nature Science Foundation [grant number 30970925 and 30730096 to W.L.]; and by the Program of Knowledge Innovation, Chinese Academy of Sciences [grant number KSCX2-YW-R-242 to W.L.].

Supplementary material available online at
http://jcs.biologists.org/lookup/suppl/doi:10.1242/jcs.086421/-/DC1

References

Björklund, A. and Dunnett, S. B. (2007). Dopamine neuron systems in the brain: an update. *Trends Neurosci.* **30**, 194-202.

Chen, H., Shalom-Feuerstein, R., Riley, J., Zhang, S. D., Tucci, P., Agostini, M., Aberdam, D., Knight, R. A., Genchi, G., Nicotera, P. et al. (2010). miR-7 and miR-214 are specifically expressed during neuroblastoma differentiation, cortical development and embryonic stem cells differentiation, and control neurite outgrowth in vitro. *Biochem. Biophys. Res. Commun.* **394**, 921-927.

Du, T. and Zamore, P. D. (2007). Beginning to understand microRNA function. *Cell Res.* **17**, 661-663.

Edbauer, D., Neilson, J. R., Foster, K. A., Wang, C. F., Seeburg, D. P., Batterton, M. N., Tada, T., Dolan, B. M., Sharp, P. A. and Sheng, M. (2010). Regulation of synaptic structure and function by FMRP-associated microRNAs miR-125b and miR-132. *Neuron* **65**, 373-384.

Hatfield, S. D., Shcherbata, H. R., Fischer, K. A., Nakahara, K., Carthew, R. W. and Ruohola-Baker, H. (2005). Stem cell division is regulated by the microRNA pathway. *Nature* **435**, 974-978.

Hébert, S. S. and De Strooper, B. (2007). Molecular biology. miRNAs in neurodegeneration. *Science* **317**, 1179-1180.

Hedlund, E., Pruszak, J., Ferree, A., Viñuela, A., Hong, S., Isacson, O. and Kim, K. S. (2007). Selection of embryonic stem cell-derived enhanced green fluorescent protein-positive dopamine neurons using the tyrosine hydroxylase promoter is confounded by reporter gene expression in immature cell populations. *Stem Cells* **25**, 1126-1135.

Houbaviy, H. B., Murray, M. F. and Sharp, P. A. (2003). Embryonic stem cell-specific MicroRNAs. *Dev. Cell* **5**, 351-358.

Jacobs, F. M., van Erp, S., van der Linden, A. J., von Oerthel, L., Burbach, J. P. and Smidt, M. P. (2009). Pitx3 potentiates Nurr1 in dopamine neuron terminal differentiation through release of SMRT-mediated repression. *Development* **136**, 531-540.

Jankovic, J., Chen, S. and Le, W. D. (2005). The role of Nurr1 in the development of dopaminergic neurons and Parkinson's disease. *Prog. Neurobiol.* **77**, 128-138.

Jomphe, C., Bourque, M. J., Fortin, G. D., St-Gelais, F., Okano, H., Kobayashi, K. and Trudeau, L. E. (2005). Use of TH-EGFP transgenic mice as a source of

identified dopaminergic neurons for physiological studies in postnatal cell culture. *J. Neurosci. Methods* **146**, 1-12.

Judson, R. L., Babiarz, J. E., Venere, M. and Blelloch, R. (2009). Embryonic stem cell-specific microRNAs promote induced pluripotency. *Nat. Biotechnol.* **27**, 459-461.

Junn, E., Lee, K. W., Jeong, B. S., Chan, T. W., Im, J. Y. and Mouradian, M. M. (2009). Repression of alpha-synuclein expression and toxicity by microRNA-7. *Proc. Natl. Acad. Sci. USA* **106**, 13052-13057.

Kawasaki, H., Mizuseki, K., Nishikawa, S., Kaneko, S., Kuwana, Y., Nakanishi, S., Nishikawa, S. I. and Sasai, Y. (2000). Induction of midbrain dopaminergic neurons from ES cells by stromal cell-derived inducing activity. *Neuron* **28**, 31-40.

Kawase-Koga, Y., Otaegi, G. and Sun, T. (2009). Different timings of Dicer deletion affect neurogenesis and gliogenesis in the developing mouse central nervous system. *Dev. Dyn.* **238**, 2800-2812.

Kim, D. W., Chung, S., Hwang, M., Ferree, A., Tsai, H. C., Park, J. J., Chung, S., Nam, T. S., Kang, U. J., Isacson, O. et al. (2006). Stromal cell-derived inducing activity, Nurr1, and signaling molecules synergistically induce dopaminergic neurons from mouse embryonic stem cells. *Stem Cells* **24**, 557-567.

Kim, J., Inoue, K., Ishii, J., Vanti, W. B., Voronov, S. V., Murchison, E., Hannon, G. and Abeliovich, A. (2007). A MicroRNA feedback circuit in midbrain dopamine neurons. *Science* **317**, 1220-1224.

Kim, J. H., Auerbach, J. M., Rodríguez-Gómez, J. A., Velasco, I., Gavin, D., Lumelsky, N., Lee, S. H., Nguyen, J., Sánchez-Pernaute, R., Bankiewicz, K. et al. (2002). Dopamine neurons derived from embryonic stem cells function in an animal model of Parkinson's disease. *Nature* **418**, 50-56.

Kim, K. S., Kim, C. H., Hwang, D. Y., Seo, H., Chung, S., Hong, S. J., Lim, J. K., Anderson, T. and Isacson, O. (2003). Orphan nuclear receptor Nurr1 directly transactivates the promoter activity of the tyrosine hydroxylase gene in a cell-specific manner. *J. Neurochem.* **85**, 622-634.

Klein, M. E., Lioy, D. T., Ma, L., Impey, S., Mandel, G. and Goodman, R. H. (2007). Homeostatic regulation of MeCP2 expression by a CREB-induced microRNA. *Nat. Neurosci.* **10**, 1513-1514.

Lee, S. H., Lumelsky, N., Studer, L., Auerbach, J. M. and McKay, R. D. (2000). Efficient generation of midbrain and hindbrain neurons from mouse embryonic stem cells. *Nat. Biotechnol.* **18**, 675-679.

Leucht, C., Stigloher, C., Wizenmann, A., Klafke, R., Folchert, A. and Bally-Cuif, L. (2008). MicroRNA-9 directs late organizer activity of the midbrain-hindbrain boundary. *Nat. Neurosci.* **11**, 641-648.

Lim, L. P., Glasner, M. E., Yekta, S., Burge, C. B. and Bartel, D. P. (2003). Vertebrate microRNA genes. *Science* **299**, 1540.

Luo, G. R., Chen, Y., Li, X. P., Liu, T. X. and Le, W. D. (2008). Nr4a2 is essential for the differentiation of dopaminergic neurons during zebrafish embryogenesis. *Mol. Cell. Neurosci.* **39**, 202-210.

Magill, S. T., Cambronne, X. A., Luikart, B. W., Lioy, D. T., Leighton, B. H., Westbrook, G. L., Mandel, G. and Goodman, R. H. (2010). microRNA-132 regulates dendritic growth and arborization of newborn neurons in the adult hippocampus. *Proc. Natl. Acad. Sci. USA* **107**, 20382-20387.

Martinat, C., Bacci, J. J., Leete, T., Kim, J., Vanti, W. B., Newman, A. H., Cha, J. H., Gether, U., Wang, H. and Abeliovich, A. (2006). Cooperative transcription activation by Nurr1 and Pitx3 induces embryonic stem cell maturation to the midbrain dopamine neuron phenotype. *Proc. Natl. Acad. Sci. USA* **103**, 2874-2879.

Nudelman, A. S., DiRocco, D. P., Lambert, T. J., Garelick, M. G., Le, J., Nathanson, N. M. and Storm, D. R. (2010). Neuronal activity rapidly induces transcription of the CREB-regulated microRNA-132, in vivo. *Hippocampus* **20**, 492-498.

Prakash, N. and Wurst, W. (2006). Genetic networks controlling the development of midbrain dopaminergic neurons. *J. Physiol.* **575**, 403-410.

Roy, N. S., Cleren, C., Singh, S. K., Yang, L., Beal, M. F. and Goldman, S. A. (2006). Functional engraftment of human ES cell-derived dopaminergic neurons enriched by coculture with telomerase-immortalized midbrain astrocytes. *Nat. Med.* **12**, 1259-1268.

Saijo, K., Winner, B., Carson, C. T., Collier, J. G., Boyer, L., Rosenfeld, M. G., Gage, F. H. and Glass, C. K. (2009). A Nurr1/CoREST pathway in microglia and astrocytes protects dopaminergic neurons from inflammation-induced death. *Cell* **137**, 47-59.

Saucedo-Cardenas, O., Quintana-Hau, J. D., Le, W. D., Smidt, M. P., Cox, J. J., De Mayo, F., Burbach, J. P. and Conneely, O. M. (1998). Nurr1 is essential for the induction of the dopaminergic phenotype and the survival of ventral mesencephalic late dopaminergic precursor neurons. *Proc. Natl. Acad. Sci. USA* **95**, 4013-4018.

Sawamoto, K., Nakao, N., Kobayashi, K., Matsushita, N., Takahashi, H., Kakishita, K., Yamamoto, A., Yoshizaki, T., Terashima, T., Murakami, F. et al. (2001). Visualization, direct isolation, and transplantation of midbrain dopaminergic neurons. *Proc. Natl. Acad. Sci. USA* **98**, 6423-6428.

Schratt, G. M., Tuebing, F., Nigh, E. A., Kane, C. G., Sabatini, M. E., Kiebler, M. and Greenberg, M. E. (2006). A brain-specific microRNA regulates dendritic spine development. *Nature* **439**, 283-289.

Sempere, L. F., Freemantle, S., Pitha-Rowe, I., Moss, E., Dmitrovsky, E. and Ambros, V. (2004). Expression profiling of mammalian microRNAs uncovers a subset of brain-expressed microRNAs with possible roles in murine and human neuronal differentiation. *Genome Biol.* **5**, R13.

Shaked, I., Meerson, A., Wolf, Y., Avni, R., Greenberg, D., Gilboa-Geffen, A. and Soreq, H. (2009). MicroRNA-132 potentiates cholinergic anti-inflammatory signaling by targeting acetylcholinesterase. *Immunity* **31**, 965-973.

Shin, D., Shin, J. Y., McManus, M. T., Ptácek, L. J. and Fu, Y. H. (2009). Dicer ablation in oligodendrocytes provokes neuronal impairment in mice. *Ann. Neurol.* **66**, 843-857.

Shioya, M., Obayashi, S., Tabunoki, H., Arima, K., Saito, Y., Ishida, T. and Satoh, J. (2010). Aberrant microRNA expression in the brains of neurodegenerative diseases: miR-29a decreased in Alzheimer disease brains targets neurone navigator 3. *Neuropathol. Appl. Neurobiol.* **36**, 320-330.

Smidt, M. P., Asbreuk, C. H., Cox, J. J., Chen, H., Johnson, R. L. and Burbach, J. P. (2000). A second independent pathway for development of mesencephalic dopaminergic neurons requires Lmx1b. *Nat. Neurosci.* **3**, 337-341.

Smrt, R. D., Szulwach, K. E., Pfeiffer, R. L., Li, X., Guo, W., Pathania, M., Teng, Z. Q., Luo, Y., Peng, J., Bordey, A. et al. (2010). MicroRNA miR-137 regulates neuronal maturation by targeting ubiquitin ligase mind bomb-1. *Stem Cells* **28**, 1060-1070.

Tiscornia, G., Singer, O. and Verma, I. M. (2006). Production and purification of lentiviral vectors. *Nat. Protoc.* **1**, 241-245.

Volpicelli, F., Caiazzo, M., Greco, D., Consales, C., Leone, L., Perrone-Capano, C., Colucci D'Amato, L. and di Porzio, U. (2007). Bdnf gene is a downstream target of Nurr1 transcription factor in rat midbrain neurons in vitro. *J. Neurochem.* **102**, 441-453.

Wayman, G. A., Davare, M., Ando, H., Fortin, D., Varlamova, O., Cheng, H. Y., Marks, D., Obrietan, K., Soderling, T. R., Goodman, R. H. et al. (2008). An activity-regulated microRNA controls dendritic plasticity by down-regulating p250GAP. *Proc. Natl. Acad. Sci. USA* **105**, 9093-9098.

Weidong, L., Conneely, O. M., He, Y., Jankovic, J. and Appel, S. H. (1999). Reduced Nurr1 expression increases the vulnerability of mesencephalic dopamine neurons to MPTP-induced injury. *J. Neurochem.* **73**, 2218-2221.

Weidong, L., Chen, S. and Jankovic, J. (2009). Etiopathogenesis of Parkinson disease: a new beginning? *Neuroscientist* **15**, 28-35.

Yekta, S., Shih, I. H. and Bartel, D. P. (2004). MicroRNA-directed cleavage of HOXB8 mRNA. *Science* **304**, 594-596.

Ying, Q. L., Stavridis, M., Griffiths, D., Li, M. and Smith, A. (2003). Conversion of embryonic stem cells into neuroectodermal precursors in adherent monoculture. *Nat. Biotechnol.* **21**, 183-186.

Yoshizaki, T., Inaji, M., Kouike, H., Shimazaki, T., Sawamoto, K., Ando, K., Date, I., Kobayashi, K., Suhara, T., Uchiyama, Y. et al. (2004). Isolation and transplantation of dopaminergic neurons generated from mouse embryonic stem cells. *Neurosci. Lett.* **363**, 33-37.

Zhao, C., Sun, G., Li, S., Lang, M. F., Yang, S., Li, W. and Shi, Y. (2010). MicroRNA let-7b regulates neural stem cell proliferation and differentiation by targeting nuclear receptor TLX signaling. *Proc. Natl. Acad. Sci. USA* **107**, 1876-1881.

Zhao, X., Tang, Y., Qu, B., Cui, H., Wang, S., Wang, L., Luo, X., Huang, X., Li, J., Chen, S. et al. (2010). MicroRNA-125a contributes to elevated inflammatory chemokine RANTES levels via targeting KLF13 in systemic lupus erythematosus. *Arthritis Rheum.* **62**, 3425-3435.